

This is a non-peer-reviewed preprint submitted to EarthArXiv.

This manuscript has been submitted to Elementa: Science of the Anthropocene

Canada's Landfill Methane Inventories: The Challenge of Accurate Modeled and Measurement-Based Emissions

Jordan Stuart (1), Evelise Bourlon (1), Rebecca Martino (1), Lindelwa Coyle (1), Susan Fraser (2), Emil Laurin (2), Felix Vogel (2), Nicholas Bishop (2), Sebastien Ars (2), David Risk (1,*)

- (1) FluxLab, Department of Earth and Environmental Sciences, St. Francis Xavier University, Nova Scotia, Canada
- (2) Environment and Climate Change Canada, Ontario, Canada

*Corresponding author: David Risk (drisk@stfx.ca)

- 1 Canada's Landfill Methane Inventories: The Challenge of Accurate Modeled and
- 2 Measurement-Based Emissions
- 3 Jordan Stuart¹, Evelise Bourlon¹, Rebecca Martino¹, Lindelwa Coyle¹, Susan Fraser², Emil Laurin², Felix
- 4 Vogel², Nicholas Bishop², Sebastien Ars², David Risk^{1,*}
- ¹FluxLab, Department of Earth and Environmental Sciences, St. Francis Xavier University, Nova Scotia,
- 6 Canada
- 7 ²Environment and Climate Change Canada, Ontario, Canada
- 8 *Corresponding author: David Risk drisk@stfx.ca

Abstract

We present a measurement-based assessment of methane emissions from 42 landfills across diverse climatic regions in Canada. Our findings reveal that emission rates predicted by the First Order Decay (FOD) model used by Environment and Climate Change Canada at the visited sites are substantially higher than most measured emission rates, on average by a factor of 3, particularly for cold and arid climates typical of the Canadian prairie provinces (by a factor of 13 on average). Bias-corrected measurement rates aligned more closely with values reported to the Canadian Greenhouse Gas Reporting Program. Compared to the amounts estimated by the FOD model, our measurement-based estimations show greater variation with changes in climate. At some warmer and wetter sites, measured rates exceeded FOD modeled estimates, underscoring the influence of climate on landfill methane dynamics and FOD model behavior. We also found that measurement-based estimates yield more realistic methane collection effectiveness values than those implied by Canada's FOD-based inventories. Our results suggest that current FOD inventory model parameters—that include decay rates and oxidation assumptions—should be refined to better reflect site-specific and climate variability.

Introduction

25

Like many countries, Canada's waste sector is a major source of methane emissions, emitting an 26 27 estimated 19 Mt CO₂e in 2023, or 0.51 t CO₂e per capita. To track greenhouse gas emissions in the waste 28 sector, Environment and Climate Change Canada (ECCC) compiles Canada's landfill methane inventory 29 using a variation of the Intergovernmental Panel on Climate Change (IPCC) First Order Decay (FOD) 30 waste model with default parameters or national, provincial, or site-level parameters when available 31 (Pipatti and Svardal, 2006). Though this model is used by ECCC to estimate emissions at the provincial level for greenhouse gas reporting in its National Inventory Report of Greenhouse Gas Sources and Sinks 32 33 in Canada (NIR), it can be configured to estimate site-specific emissions by incorporating available 34 operational information, waste tonnage, waste composition, decay rate, and methane generation potential. 35 Calculation of methane emission is based on modeled methane generation adjusted for any methane 36 destruction (accounting for flaring efficiency) or utilization and methane oxidation of the generated 37 methane that is not recovered in landfill covers (the IPCC default oxidation factor of 0.1 is used for all 38 regions and years; ECCC, 2025). At municipal solid waste landfills, the emission uncertainty was 39 estimated to be $\pm 76\%$ using the default parameters from the IPCC 2006 Guidelines (IPCC, 2006). Gaps in 40 input activity timeseries are completed with interpolated or extrapolated values (ECCC, 2025). 41 In addition to compiling Canada's methane inventory, ECCC administers Canada's Greenhouse Gas 42 Reporting Program (GHGRP). Landfills emitting 10 kt CO₂e/year or more are required to report 43 emissions to the GHGRP. However, unlike in the United States, where GHGRP data are integrated into 44 its national inventory estimates (EPA, 2023), Canada uses them to compare and validate its inventory. Canadian landfills reporting to the GHGRP are not required to use a standard methodology. Some 45 operators rely on engineering calculations using the IPCC FOD model or alternatives such as the United 46 47 States Environmental Protection Agency's LandGEM model.

Differences in methodology contribute to observed discrepancies between operator-reported GHGRP values and the ECCC's IPCC-based estimates. Based on our subset of landfills, the ECCC-modeled emissions are typically higher on a site-by-site basis—sometimes only marginally, but in some cases, more than nine times higher. Such inconsistencies are increasingly problematic because national inventories face government and public scrutiny. Discrepancies between modeled and measured landfill methane emissions are well-documented, with international studies reporting underestimations of up to 200% in individual and governmental inventories (Wang et al., 2024; Scarpelli et al., 2024; Cusworth et al., 2024). In the United States, two recent studies found that measured emissions exceeded American GHGRP-reported values in 47% of cases and were, on average, 2.7 times higher across all American landfills (Scarpelli et al., 2024; Cusworth et al., 2024). In Canada, Thompson et al. (2009) found that the Scholl Canyon model often overestimated methane recovery rates, and LandGEM consistently underestimated them. Smaller landfills have also overestimated methane inventories due to modeling limitations (Sharff and Jacobs, 2006). The inaccuracy of waste models is due to several factors. Many landfill methane models rely on environmental parameters that are challenging to validate, and models often fail to account for seasonal and climatic variability (Gollapalli and Kota, 2018). For example, Scheutz et al. (2011) reported lowerthan-expected methane emissions in Denmark due to precipitation patterns, temporal variability, and landfill characteristics. Similarly, Jain et al. (2021) observed lower emissions from landfills in arid regions compared to wetter climates. Among our selected sites, six of the ten most significant differences between ECCC modeled emissions and GHGRP reports are from Alberta and Saskatchewan, regions where annual precipitation may be as low as 250 mm. Effectively mitigating methane depends on accurate inventories so that interventions can be identified and prioritized. In its National Inventory Report (ECCC, 2025), ECCC acknowledges landfill methane emissions as the largest source of uncertainty at the national level. Draft regulatory language has been released to reduce waste-sector methane, but the ability to accurately measure the impact of regulations will depend on how well landfill

48

49

50

51

52

53

54

55

56

57

58

59

60

61

62

63

64

65

66

67

68

69

70

71

methane emissions and their sources can be quantified. Reducing inventory uncertainty will require improving the quality of the FOD model input data from Canada's approximately 270 large landfills, which account for more than 85% of Canada's methane landfill emissions (ECCC, 2022). Furthermore, improving data collection will enhance model validation capabilities. This study compares measurement-based landfill methane emission rates to those modeled by ECCC using the IPCC FOD model and those reported to GHGRP. We also examine the influence of climate variability on measured emissions, considering factors such as the accumulated waste size and the effectiveness of methane collection systems. Methods Site Locations

From July to November 2022, we surveyed landfills across Canada, with or without methane collection systems, varying in size and operational status (open or closed). For our analysis, we focused on 42 sites (Figure 1) where we had obtained off-site emission rate estimates under the following conditions: wind speeds within an appropriate range, an unobstructed line of sight to the landfill, and no issues with measurement instrumentation.

Measurements

For the landfill emission measurement campaign, we used a mobile survey laboratory. The mobile laboratory consisted of a Toyota RAV4 outfitted with a Picarro gas analyzer (G2210-i CRDS, Picarro Inc., USA) connected to a high-volume 7 LPM pre-pump. The setup minimized the lag time between the external air inlet and the instrument. At the front of the vehicle, we mounted the air inlet on a mast fixed to the vehicle's roof. An open Y-splitter fitting allowed excess airflow to be released. The mast also housed a 2-axis ultrasonic anemometer (WindSonic, Gill Instruments Ltd, UK), an electric compass

95 (Model 32500, RM Young, USA), and a GPS (18x, Garmin Ltd, USA). All mast-mounted equipment was 96 approximately 2.5 m above ground level. A data logger (CR1000X, Campbell Scientific, USA) recorded 97 all measurements, including internal time, at 2 Hz. 98 Before and after the field campaign, we benchmarked the Picarro analyzer using calibration gases of 99 known composition from the AmeriFlux Management Program (Lawrence Berkeley National Laboratory, 100 Berkeley, CA, USA). These gases contained dry natural air calibrated to the World Meteorological 101 Organization mole fraction scales for carbon dioxide (X2019) and methane (X2004a). We determined the 102 instrument offset by having compressed gas flow through the analyzer for over a day until H₂O levels 103 stabilized below 0.05%. When the methane offset exceeded 10 ppb, we recalibrated the analyzer. We 104 repeated this process at the end of each field campaign to verify the stability of the calibration. 105 During fieldwork, we conducted a second daily check: each morning, we benchmarked the Picarro 106 analyzer with a target gas containing known CO₂ and CH₄ mixing ratios. The cylinder was attached for 107 five minutes to monitor any deviation between the known and measured values. While field benchmarks 108 are inherently more variable than laboratory tests, our field benchmarks were sufficient for detecting 109 major drift, which we did not observe. 110 Each morning, we also measured the lag time between the inlet and analyzer cavity by introducing CH₄ pulses at the inlet and timing how long it took the pulses to arrive at the analyzer. The measured lag time 111 112 ensured that the gas mixing ratio measurements with the GPS locations were precisely aligned. To 113 confirm that the slower response time of the Picarro G2210-i adequately captured plumes, we compared 114 our measurements with the measurements of two faster analyzers, a Licor LI7810 and a Picarro G2401, 115 used in a simultaneous companion survey conducted by ECCC. While our Picarro damped peak CH₄

values and extended plume duration, the areas under the curve were equal between the analyzers (Figures

116

117

S1 and S2).

We conducted downwind transect measurements across one or multiple plumes, progressing from background levels to peak values and back. We repeated each transect up to 15 times at speeds ranging from 15 to 80 km/h, depending on safety and traffic conditions. When operators granted us landfill access, we also conducted on-site measurements to better characterize potential emission sources. However, in this study, we only used the off-site downwind measurements to estimate emission rates. Data Processing and Selecting Transects Following the data quality checks, we calculated true wind vectors using measured wind speeds, compass readings, and GPS data. We calculated the Sun's position and collected meteorological data from the nearest airport that included cloudiness, ceiling height, and wind to estimate atmospheric stability classes using Turner's method (Turner, 1964). We excluded transects collected when wind speeds were less than 1.5 m/s, during highly unstable conditions (Pasquill stability class "A"), or during the night (Pasquill stability classes "E" and "F"). We estimated the ambient methane level using iterative mean suppression (Liland, 2015), and we defined methane enhancements to be the difference between measured and ambient levels. We discarded the transects that had no significant plume (enhancement <0.01 ppm). We mapped and assessed the remaining transect locations relative to landfill boundaries. Using Google imagery and Street View, we identified potential obstacles to dispersion (e.g., tall buildings or dense forests) and screened for nearby non-landfill methane sources such as dairy and poultry farms, compost facilities, water treatment plants, cattle exchange centers, and oil and gas infrastructure. We excluded the transects influenced by such obstacles or additional methane sources. Finally, we calculated the distance between each landfill and its associated methane enhancements, retaining only transects where this distance was less than 2.5 km.

Estimating Emission Rates

118

119

120

121

122

123

124

125

126

127

128

129

130

131

132

133

134

135

136

137

138

139

To estimate the landfill emission rates from the measured methane enhancements, we used a Gaussian dispersion model. Gaussian dispersion models are widely used to simulate air pollutant dispersion and have effectively estimated biogas emissions from landfills (Fredenslund et al., 2019; Aronica et al., 2009). While Gaussian methods are somewhat less accurate than tracer gas approaches, they are faster to implement, do not require site access, and cost roughly two-thirds less, making them well-suited for screening studies like ours (Fredenslund et al., 2019; Fallah-Shorshani et al., 2017; Matacchiera et al., 2019). Many Canadian landfills are in remote areas with limited road networks, often forcing transects to be near landfill fence lines where multiple Gaussian peaks have been observed because several methane sources within a landfill operation are present (Cusworth et al., 2024). In contrast to Fredenslund et al. (2019), we found that it was not always possible to model a completely coalesced plume or to assume the landfill center was the main source of methane. In our case, we did not know the source locations and emission rates. Our approach was like that of Gillespie et al. (2025) and Ars et al. (2020), which involved minimizing differences between the observed enhancements and Gaussian model predictions. Unlike Gillespie's approach, which used either the known centers of emitting features of the landfill or the corners of the landfill as potential emitting sources, we used random sets of potential emitting points sampled from gridded locations within landfill boundaries, and then we simultaneously calculated their emission rates. Both Gillespie's approach and ours were tested concurrently at a controlled methane release site, producing similar rate estimates (Hossain, 2025). The Gaussian model accounted for parameters including source-measurement distances, source and measurement heights above ground, wind speed, and dispersion coefficients (sigma parameters). We assumed that the corrected wind at the measurement location reflected the wind at the source, and that the source emissions were continuous. We derived the dispersion parameters from the Pasquill-Gifford-Turner model for open-country settings, based on atmospheric stability. Our algorithm estimates the total landfill emission rate by adjusting the contribution from each source to ensure that the sum of modeled methane concentrations matches the

141

142

143

144

145

146

147

148

149

150

151

152

153

154

155

156

157

158

159

160

161

162

163

164

measured methane enhancements. More information on the Gaussian Plume Model and the inversion is available in the Supporting Information. We retained only those results for which the total modeled methane enhancement fell between 80% and 200% of the measured enhancement along downwind transects. We calculated the total landfill emission rates by summing the individual source rates. We repeated this operation over 1000 random distributions of sources, and each landfill was attributed the average and standard deviation of the estimated rate ensemble.

Atmospheric conditions, such as wind and stability class, can influence the uncertainties in emission rate estimates. Landfills, due to their topography and heat generation, often create localized microclimates, which means that meteorological parameters measured on nearby roads or at airports might not perfectly represent conditions at the emission sources. We analyzed emissions assuming fixed source heights (4 m above road level) and variable heights from high-resolution digital elevation models (HRDEM; Natural Resources Canada) but found no significant differences in estimated rates. Source height was not a critical parameter when measurements were taken hundreds of meters from the sources.

To evaluate uncertainty and bias, we conducted a controlled release experiment at a closed landfill with a gas collection system. This included 35 double-blind tests downwind of eight point sources and two area sources (>200 m²) spread over 10 ha, emitting 25 kg/h to 250 kg/h. Our method consistently captured 66% of true emissions, with an uncertainty of ±47.6% across rates from 0 kg/h to 238 kg/h (Hossain et al., 2025). When measurements were collected nearly 2.5 km away or with forested obstacles between the landfill and the mobile laboratory, the resulting emission rates of the controlled release experiment tended to be underestimated. To minimize underestimating the emissions rates in this study, we avoided having distant transects and obstructed lines of sight.

We present the emission rate estimates directly from the Gaussian inversion and as bias-corrected values (adjusted by 1/0.66). Fredenslund et al. (2019) observed a similar downward bias, reporting a factor of

0.72 when they validated a Gaussian model using tracer-gas-correlation results in a study involving 91 landfills across Denmark.

Landfill categories

We categorized landfills by area and climate. For landfill size binning, we divided the 42 landfills into three equal groups—small, medium, and large—based on each site's accumulated methane generation potential as calculated by ECCC (Figure 2). For climate classification, we initially used Köppen climate zones, but found most landfills clustered within a single zone, in particular, the humid continental zone. To refine the classification, we extracted weather data from local ECCC stations within 50 km of each landfill, including daily or hourly precipitation (rain and snow) and temperature records from 2018 to 2022. From these data, we calculated annual total precipitation and mean air temperature. Plotting temperature versus precipitation enabled us to visually cluster the site into five climate categories (see the cluster extents on Figure 2):

- lower precipitation and lower temperature,
- lower precipitation and mid temperature,
- mid precipitation and higher temperature,
- higher precipitation and mid temperature, and
- much higher precipitation and/or much higher temperature.

These categories are relative to our dataset of 42 landfills, for which we defined "much higher" temperature as having an annual mean temperature above 10°C and "much higher" precipitation as over 1750 mm/year; they are only based on the visual inspection of Figure 2, and not based on Canada's or the world's climate zones. When mapped (Figure 1), these categories revealed meaningful geographic patterns, with wetter climates concentrated near the west and east coasts and colder climates at northern latitudes.

Comparing Measurement Estimates with FOD Modeled Values

Unlike the ECCC and GHGRP annual emission estimates, our measurement-based rates represent instantaneous ("snapshot") landfill emissions, primarily during summer (38 sites visited during summer; 6 during fall). Canada's extreme seasonality means summer temperatures can exceed winter values by more than 30°C. The seasonal variability calls into question some of the parameterization of the First Order Decay model. At all sites, ECCC includes a 10% methane oxidation factor on the portion of methane that is not collected to account for methanotrophs in landfill biocovers reducing fugitive methane emissions. This is the default IPCC oxidation value, based on studies by Czepiel et al. (1996a, b) at a New Hampshire landfill. It represents an annual average, with actual oxidation likely negligible in winter but potentially high in summer. Optimal oxidation rates are reported at 25°C to 35°C (Spokas and Bogner, 2011), but methanotrophs can utilize CH₄ at far lower temperatures with an optimal temperature of 3.5°C to 10°C (Omelchenko et al., 1993), and methanotrophic activity has been observed at 1-2°C (Scheutz and Kjeldsen, 2004; Einola et al., 2007). Chanton et al. (2009, 2011) found annual oxidation fractions ranging from 11% to 89%, with a mean of 35%. To account for this, we compared measurement estimates to the standard ECCC modeled rates (10% oxidation) and to an adjusted model assuming a higher oxidation of 35%. We are not suggesting that the oxidation rate is 35% during the summer in Canada; instead, we use this percentage as another point for comparison. We calculated the adjusted ECCC modeled emission rates by dividing original model estimates by ~ 1.4 [(1-0.1)/(1-0.35)].

Results

212

213

214

215

216

217

218

219

220

221

222

223

224

225

226

227

228

229

230

231

232

233

234

On-site Observations

We gained access to 50% of the sites, which allowed us to better characterize methane sources and identify landfill areas with the highest emissions. Across these sites, the largest emissions were consistently observed at the active working faces, where new waste was deposited daily. These areas

typically lacked covers and had not been integrated into landfill gas collection systems, making them major contributors to fugitive methane. Beyond the active working faces, we recorded elevated methane levels around manholes and leachate wells. In some cases, we also detected methane peaks downwind of compost piles during humid weather; however, compost-related emissions were low or absent. Furthermore, we found that operational activities influenced emission patterns. We measured the highest on-site methane mixing ratios during construction activities, such as the installation of landfill gas collection systems, manholes, and leachate wells. These locations frequently produced methane levels high enough to saturate our analyzer (30 ppm). Occasionally, we were on site when leachate wells were being emptied, and at these times, we observed significant methane spikes.

Comparing our Measurement-based Values to ECCC Modeled Values and GHGRP Industry-Reported Values

We obtained ECCC modeled annual methane emission rates for 2022 at 40 of the 42 sites and emission rates for 2021 for 2 landfills. It should be noted that the 2021 modeled rates are based on a slightly different input parameter estimation approach, although they are derived from the same IPCC FOD model. The ECCC dataset also included reported methane flaring and collection amounts from a voluntary survey of landfill operators conducted by ECCC, and estimations of methane generation potential (L₀ in tons of CH₄), especially the accumulated L₀ that accounts for L₀ remaining in the landfill after previous decay and is used as a proxy for the landfill size in this study. The L₀ represents the potential amount of methane that could be generated from the landfill waste. Of 42 landfills, 31 reported flared and/or utilized methane amounts in 2022. It is unclear whether the sites for which we lack this information do not have a collection system or simply did not report it. We collected industry-reported emission rates for 2022 from the Canadian GHGRP database for 33 of the 42 sites. The ECCC rates were consistently the highest of the two types of rates, ranging from near 0 kg/h to 2368 kg/h (mean: 471 kg/h), whereas the GHGRP rates ranged from 36 kg/h to 1511 kg/h (mean: 357 kg/h). With an oxidation rate of 35%, the ECCC rates range from near 0 kg/h to 1710 kg/h, with a mean of 340 kg/h, closer to the

GHGRP range. Our direct measurement-based rates were generally lower than the ECCC or GHGRP rates, ranging from 3 kg/h to 511 kg/h with a mean of 118 kg/h. When we applied the bias correction from the controlled release experiment, our adjusted rates ranged from 5 kg/h to 774 kg/h (mean: 179 kg/h). The GHGRP and ECCC rate distributions had a primary mode at 178 kg/h, whereas the measurementbased rate distribution peaked at 30 kg/h (Figure 3). However, the bias-corrected measurement-based distribution and GHGRP distribution shared a secondary mode from around 690 kg/h to 750 kg/h. The ECCC emission rates exceeded 39 direct measurement-based rates and 37 bias-corrected measurement-based rates out of 42 sites (resp. 93% and 88%) and were higher than the GHGRP-reported rates for 20 of 33 sites (61%). In contrast, direct measurement-based rates surpassed GHGRP-reported values for only 4 of 33 sites (12%), and bias-corrected rates exceeded GHGRP values for 9 of 33 sites (27%). The five sites where our bias-corrected estimated rates exceeded the ECCC modeled rates are all in wet climate categories. Of the five, two have similar rates, with a difference of less than 10kg/h. For the three other sites, the ECCC modeled rates are also lower than the GHGRP rates. We found that the highest emission rates were from open landfills. Of the 42 sites we visited, 9.5% (4) sites) were closed; that is, they no longer accepted waste and had completed final covers and landscaping. Some of these closed sites had been repurposed for recreational use (e.g., golf courses, dog parks). At closed sites, we observed relatively low bias-corrected emission rates (11 kg/h to 244 kg/h), which were close to ECCC FOD estimates (near 0 kg/h to 257 kg/h). However, for two of three closed sites, operators reported unusually high values to the GHGRP (449 kg/h and 779 kg/h), exceeding our measurementbased and the ECCC modeled estimates. For subsequent analyses, we focused on the bias-corrected values because they compared more favorably to "true" emissions (i.e., the true release rates of the controlled release experiment by Hossain et al. (2025)) on the measurement days without altering patterns relative to the ECCC modeled or GHGRP values. On average, the ratio of the ECCC rates to the measurement-based rates was 3.3 for closed sites

260

261

262

263

264

265

266

267

268

269

270

271

272

273

274

275

276

277

278

279

280

281

282

(mean difference: 57 kg/h) and 6.4 for open sites (mean difference: 317 kg/h). Overall, the bias-corrected measurement-based rates aligned more closely with GHGRP values (R² = 0.636, slope = 0.529) than with the ECCC FOD estimates (R² = 0.627, slope = 0.335) (Figure 4). Adjusting the ECCC FOD estimates for 35% oxidation improved the comparison with our measurement-based rates (R² = 0.627, slope = 0.463; Figure 4). However, when their respective uncertainties are accounted (76% for ECCC and 47.6% for measurement-based estimates), ECCC and measurement-based emission rate estimate ranges overlap, except for a few landfills located in the drier areas of our study.

284

285

286

287

288

289

290

291

292

293

294

295

296

297

298

299

300

301

302

303

304

305

306

307

308

It should be noted that our measurements assessed only the emitted methane, not the methane produced (the sum of the methane emitted, collected, and oxidized). Landfill operators report the amount of methane flared and/or utilized to ECCC, but we do not know the amount of oxidized methane. Therefore, we calculated methane collection effectiveness (collected / emitted+collected) instead of collection efficiency (collected/produced). Lower measurement-based rates resulted in higher calculated collection effectiveness, with a median of 51% overall and 76% for the large landfills, consistent with engineering expectations for systems installed on covered landfill areas. In contrast, we found the collection effectiveness derived from the ECCC FOD estimates to be substantially lower, with a median of 20% overall and 52% for the large landfills (Figure 5). The greater efficiency observed at the largest sites (in terms of accumulated waste) may be attributed to their higher collection system coverage, as they have a larger ratio of closed cell area to active cell area compared to smaller sites. Figure 6 shows the distribution of effectiveness for two types of climates: "dry", which combines the two lower precipitation categories, and "wet", which comprises the mid, high, and higher precipitation climate categories. The measurement-based emission rates do not lead to any difference in effectiveness, with a similar range and the same median. However, the ECCC emission estimates suggest a large difference in effectiveness, with a lower effectiveness at "dry" sites than at "wet" sites.

As shown in Figure 7, relative to measurement-based rates, the ECCC underpredicts emissions in the warmest, wettest areas (the west coast). However, in drier climates, particularly Canada's arid central

regions, the measurement-based rates diverged sharply from the ECCC FOD estimates, which are, on average, over 12 times higher than the measured rates.

Discussion

309

310

311

312

313

314

315

316

317

318

319

320

321

322

323

324

325

326

327

328

329

330

331

332

The key finding of this study is that measurement-based summer snapshots of methane emissions at Canadian landfills are lower than the annual emissions predicted by the ECCC FOD modeled emissions. This divergence reflects a combination of factors: potential bias in the measurement technique, unrealistic model parameters, or both. Our rates were derived from field surveys conducted primarily during the summer with warm air temperatures and low wind speeds. Barometric pressure and temperature were measured at only a few landfills where sensor towers could be deployed, so these sparse records do not allow us to conclude anything about the influence of atmospheric pressure or temperature. In their 2025 study, Gillespie et al. examined how these drivers could affect measurement-based emission estimates at landfills in Ontario. They found that inclusion of these drivers improves the slope of the best-fit line compared to inventoried emissions, though it does not significantly alter the correlation coefficients. However, methane oxidation by landfill cover layers could be more effective during summer, when our surveys were conducted, than during winter, and could be higher than the 10% default annual oxidation factor assumed in the ECCC FOD modeling. Methanotroph activity depends on landfill cover characteristics and increases with temperature (Börjesson and Svensson, 1997; Park et al., 2005). Although cover properties vary among landfills and with environmental conditions, oxidation can be a significant factor in the differences between our measurement-based rates and ECCC FOD estimates, underscoring the importance of methanotrophs and covers in reducing landfill emissions. This study also highlights the limitations of applying default or large-scale model parameters, especially decay rates (k), across Canada's diverse climate zones to model the methane generation at each landfill. Our measurement-based estimates were substantially variable depending on the climate zone. Figure 8 illustrates methane generation (emitted + 10% oxidized + recovered) per accumulated methane generation potential L₀ for each climate category. The CH₄ generation potential L₀ (in tonnes of CH₄) is estimated from the mass of degradable organic matter multiplied by the fraction of landfill gas that is CH₄ (1/2) and the molecular weight ratio of CH₄ over C (16/12). Note that this L_0 definition is different from the one provided in the IPCC 2000 Good Practice Guidance, where it is expressed as tonnes of methane per tonnes of waste landfilled. The accumulated methane generation potential L_0 accounts for the previous year's L₀ decay. In the ECCC modeling, the amount of degradable organic matter is based on waste composition determined at the provincial level, not the site level, and does not account for any sitespecific variability. As a result, ECCC might overestimate methane production at large urban landfills where organic waste diversion programs are active. Figure 8 illustrates the contrast between measurement-based methane generation per methane generation potential L₀, which increases as the climate gets wetter and warmer, and the ECCC FOD-based methane generation, which displays bimodal variability—showing a similar amount at all the drier sites and a different, consistent amount at all the wetter sites. The measurement-based methane generation is lower than the model-based values except for the wettest climate zone. This could be an indication of a potential overestimation of the methane generation, hence the methane emission, especially in low precipitation areas. There is no clear relationship with the amount of landfill waste. Assuming a methane generation time of 15 years followed by negligible generations, the measurementbased methane generation translates to a methane generation potential from the measurement-based rates of 1 m³ to 56 m³ CH₄ per tonne of total accumulated waste (the annual total amount of waste that remains after some water removal and decomposition), and 27 m³ and 33 m³ CH₄ per tonne of accumulated waste from ECCC FOD modeled methane generation for "dry" and "wet" climate respectively. In a review by Krause et al. (2016), methane generation potentials ranged from 20 m³ to 223 m³ CH₄ per tonne of municipal solid waste. Our values and ECCC values fall within the lower quarter of this range, which we expect for dry and cold Canadian conditions. However, ECCC values are higher than measurement-based

333

334

335

336

337

338

339

340

341

342

343

344

345

346

347

348

349

350

351

352

353

354

355

356

357

values for all but the wettest and/or warmest sites.

The ECCC FOD estimates have a pronounced upward bias for cold and arid climates and underestimate emissions for the warmer and/or wetter areas (Figure 7). Vu et al. (2017) demonstrated that FOD models with default parameters fail to capture methane production dynamics for cold semi-arid climates, with mean percentage errors ranging from 55% to 135%. We estimated the bulk landfill waste decay rates (k) both from our measurements, assuming a 10% methane oxidation, and the FOD-modeled rates, as:

358

359

360

361

362

363

364

365

366

367

368

369

370

371

372

373

374

375

376

377

378

379

$$k = -\ln\left(1 - \frac{emitted + collected + oxidized}{L_0}\right). \tag{1}$$

The values are reported in Table A. Decay rates vary widely by waste composition and moisture content, and nutrient availability, pH, and temperature are less significant factors. Our median k values vary from 0.004 to 0.0063 y⁻¹, from the coldest, driest sites to the warmest, wettest sites. The FOD-based k values, accounting for regional waste composition, are 0.03 y⁻¹ for the dry sites and 0.05 y⁻¹ for the wet sites. The values range within the range reported by Jain et al. (2021) from a study of 114 landfills in the United States, from 0.004 to 0.226 y⁻¹, with a median of 0.068 y⁻¹. Both Canadian FOD and measurement-based k values fall within the lower half of the US k value range. This may be due to factors such as lower temperatures, prolonged sub-zero periods, reduced precipitation, and differences in waste composition resulting from distinct organic diversion practices. The measurement-based k values indicate that waste decay is significantly slower under dry and cold conditions than assumed by the FOD model. This disparity may be further amplified because our measurements were taken during the summer, which can be drier than other seasons and may affect waste moisture levels. The default IPCC bulk waste decay rate values—0.05 y⁻¹ for boreal/temperate dry climates and 0.09 y⁻¹ for boreal/temperate wet climates—are, on average, 1.7 times higher than the ECCC FOD values and over 3 times higher than the measurementbased estimates. More accurate decay rates and methane generation potentials tailored to Canadian climate zones could improve inventory estimates and scale them downward. Given Canada's rapidly changing climate, understanding methane generation under different environmental conditions is critical.

Our findings emphasize the need for models to reflect the landfill dynamics associated with site specificity in each region to accurately assess gas collection system performance. Based on our measurement-based emission rates, the median collection effectiveness was 51%, aligning with studies by Duan et al. (2022), who reported a range of 13% to 86% and a mean of 50% at Danish landfills using the same effectiveness definition (i.e., no oxidation accounted). In contrast, the ECCC FOD model estimates suggested an average collection effectiveness of only 20%, implying that collection systems were far less effective than they were in practice. Extrapolating annual emissions from single-day measurements introduces uncertainty due to diurnal and seasonal variability in landfill emissions. However, models also require credible annual parameters that reflect landfill management and climate. Repeated measurements over multiple days, seasons, and years would improve accuracy and confidence. Our research contributes to a growing body of work informing inventory refinement and demonstrates the value of measurement-based approaches in optimizing model parameters and reducing uncertainty. Improving regulatory data collection from landfill operations and waste composition would further reduce uncertainty and support evidence-based policy development. Canada's regulatory plan (Government of Canada, 2024) aims to reduce landfill methane emissions by 50% below 2019 levels by 2030, through a new regulated framework based on surface methane concentration thresholds. Methane mitigation measures include the implementation or expansion of landfill methane control approaches such as landfill gas recovery systems, engineered biosystems, or methane destruction devices. Currently, about 150 large landfills in Canada have gas recovery systems, and expanding their installation at more sites could be a significant step. However, engineering calculations often assume 75% and 90% collection efficiency for open and closed sites, respectively, which are much higher percentages than the one estimated from both measurement and FOD modeling.

We hypothesize that active working face emissions, which can account for up to half the total landfill

emissions and typically lack collection infrastructure (Scarpelli et al., 2024; Risk et al., 2025), might be

overlooked. Without strategies that address active working faces and/or landfill methane reduction

380

381

382

383

384

385

386

387

388

389

390

391

392

393

394

395

396

397

398

399

400

401

402

403

measures that account for lower collection efficiencies, Canada could fall short of its 50% reduction goal. Because of lower efficiency, collection systems might need to be deployed at a larger number of sites than planned. However, the goal could be achieved if the reduction strategies were complemented by policies incentivizing active face collection. While only two landfills in Canada currently use active face collection systems, the technology is widely deployed in countries like the United Kingdom and could be scaled for use in Canada.

On a positive note, our measurements suggest that landfill methane emissions in the Canadian inventory tend to be overestimated. Emissions from arid regions were notably overpredicted. Our bias-corrected measurements, while offering a snapshot at a limited number of Canadian landfills, indicated that landfill methane inventories could be overstated by at least a factor of two, given the distribution of landfills across Canada.

The Canadian government has already demonstrated a commitment to inventory accuracy by implementing a measurement-informed methane inventory for the oil and gas sector—the first of its kind globally—by incorporating extensive aircraft site measurements annually to verify inventory estimates. A similar approach could be applied to the waste sector, where fewer sites and highly accurate methods, such as the ground-based tracer gas method, could make the initiative feasible and impactful.

Conclusion

This study provided a measurement-based assessment of methane emissions from Canadian landfills on a national scale, revealing systematic discrepancies between ECCC estimates based on the IPCC FOD model and the measurement-based estimates. Our findings showed that the ECCC modeling often overestimates emissions from cold and arid regions, while occasionally underestimating emissions from warmer, wetter climates. These mismatches highlight the need to refine inventory parameters, such as

decay rates and oxidation assumptions, to better reflect Canada's climate diversity and site-specific landfill practices.

By integrating bias-corrected mobile survey measurements with regulatory data, we demonstrated that Canada's landfill methane inventory might be overstated—potentially by a factor of two. This suggests that methane mitigation targets could be more achievable than anticipated, especially if active work faces and other high-emitting sources were effectively managed. However, improving inventory accuracy requires measurement campaigns, not necessarily similar to the survey approach used in this exploratory study, at a selection of sites that reflect all the landscape and climatic conditions encountered in Canada, and better regulatory data on landfill operations and waste composition to improve the input parameters of FOD models. Tracking emissions over an extended period at certain sites would provide valuable insights into how factors like weather or operational changes impact emission variability. As Canada moves towards ambitious waste sector methane reduction targets, aligning mitigation strategies with measurement-informed inventories will be critical to success. Our study underscores how valuable empirical data can be for validating models and supporting the case for scaling up measurement-informed approaches—already pioneered in Canada's oil and gas sector—to achieve similar transparency and effectiveness in waste management.

- 444 References
- Aronica, S, Bonanno, A, Piazza, V, Pignato, L, Trapani, S. 2009. Estimation of biogas produced by the
- landfill of Palermo, applying a Gaussian model. Waste Management 29(1): 233–239.
- 447 https://doi.org/10.1016/j.wasman.2008.02.026
- 448 Ars, S, Vogel, F, Arrowsmith, C, Heerah, S, Knuckey, E, Lavoie, J, Lee, C, Pak, NM, Phillips, JL,
- Wunch, D. 2020. Investigation of the Spatial Distribution of Methane Sources in the Greater Toronto
- 450 Area Using Mobile Gas Monitoring Systems. *Environmental Science and Technology* 54(24): 15671–
- 451 15679. https://doi.org/10.1021/acs.est.0c05386
- Börjesson, G, Svensson, BH. 1997. Seasonal and diurnal methane emissions from a landfill and their
- regulation by methane oxidation. *Waste Management and Research* 15(1): 33–54.
- 454 https://doi.org/10.1006/wmre.1996.0063
- 455 Chanton, JP, Powelson, DK, Green, RB. 2009. Methane Oxidation in Landfill Cover Soils, is a 10%
- 456 Default Value Reasonable? *Journal of Environmental Quality* 38(2): 654–663.
- 457 https://doi.org/10.2134/jeq2008.0221
- Chanton, J, Abichou, T, Langford, C, Spokas, K, Hater, G, Green, R, Goldsmith, D, Barlaz, MA. 2011.
- Observations on the methane oxidation capacity of landfill soils. *Waste Management* 31(5): 914–925.
- 460 https://doi.org/10.1016/j.wasman.2010.08.028
- Cusworth, DH, Duren, RM., Ayasse, AK, Jiorle, R, Howell, K, Aubrey, A, Green, RO, Eastwood, ML,
- Chapman, JW, Thorpe, AK, Heckler, J, Asner, GP, Smith, ML, Thoma, E, Krause, MJ, Heins, D,
- 463 Thorneloe, S. 2024. Quantifying methane emissions from United States landfills. *Science* 383(6690):
- 464 1499–1504. https://doi.org/10.1126/science.adi7735

Czepiel, P. M., Mosher, B., Crill, P. M., & Harriss, R. C. (1996a). Quantifying the effect of oxidation on 465 466 landfill methane emissions. Journal of Geophysical Research: Atmospheres, 101(D11), 16721–16729. https://doi.org/10.1029/96JD00222 467 468 Czepiel, P. M., Mosher, B., Harriss, R. C., Shorter, J. H., McManus, J. B., Kolb, C. E., Allwine, E., & 469 Lamb, B. K. (1996b). Landfill methane emissions measured by enclosure and atmospheric tracer 470 methods. Journal of Geophysical Research: Atmospheres, 101(D11), 16711–16719. https://doi.org/10.1029/96JD00864 471 Duan, Z, Kjeldsen P, Scheutz, C. 2022. Efficiency of gas collection systems at Danish landfills and 472 implications for regulations. Waste Management 139: 269–278. 473 474 https://doi.org/10.1016/j.wasman.2021.12.023 475 Einola, J.-K. M., Kettunen, R. H., & Rintala, J. A. (2007). Responses of methane oxidation to temperature and water content in cover soil of a boreal landfill. Soil Biology and Biochemistry, 39(5), 1156–1164. 476 477 https://doi.org/10.1016/j.soilbio.2006.12.022 478 Environment and Climate Change Canada. 2022. Reducing methane emissions from Canada's municipal 479 solid waste landfills: Discussion paper. https://www.canada.ca/en/environment-climatechange/services/canadian-environmental-protection-act-registry/reducing-methane-emissions-480 canada-municipal-solid-waste-landfills-discussion.html 481 482 Environment and Climate Change Canada. 2025. National Inventory Report 1990-2023: Greenhouse Gas Sources and Sinks in Canada. Available online at: canada.ca/ghg-inventory. 483 484 EPA (2023) Inventory of U.S. Greenhouse Gas Emissions and Sinks: 1990-2021. U.S. Environmental 485 Protection Agency, EPA 430-R-23-002. https://www.epa.gov/ghgemissions/inventory-us-greenhousegas-emissions-andsinks-1990-2021. 486

487	Fallah-Shorshani, M, Shekarrizfard, M, Hatzopoulou, M. 2017. Integrating a street-canyon model with a
488	regional Gaussian dispersion model for improved characterisation of near-road air pollution.
489	Atmospheric Environment 153: 21–31. https://doi.org/10.1016/j.atmosenv.2017.01.006
490	Fougère, CR, Ghasemi, D, Khaleghi, A, Coyle, L, Bourlon, E, Li, H, Smith, M, Risk, D. 2025. Estimating
491	Canadian landfill methane emissions from aircraft measurements [preprint]. Social Science Research
492	Network. https://doi.org/10.2139/ssrn.5186900
493	Fredenslund, AM, Mønster, J, Kjeldsen, P, Scheutz, C. 2019. Development and implementation of a
494	screening method to categorise the greenhouse gas mitigation potential of 91 landfills. Waste
495	Management 87: 915–923. https://doi.org/10.1016/j.wasman.2018.03.005
496	Gillespie, LD, Ars, S, Alkadri, S, Urya, S, Khoo, T, Fraser, S, Vogel, F, Wunch, D. 2025. Estimating
497	methane emissions from the waste sector in Southern Ontario using atmospheric measurements.
498	Journal of the Air and Waste Management Association 75(2): 144–163.
499	https://doi.org/10.1080/10962247.2024.2435340
500	Gollapalli, M, Kota, SH. 2018. Methane emissions from a landfill in north-east India: Performance of
501	various landfill gas emission models. Environmental Pollution 234, 174–180.
502	https://doi.org/10.1016/j.envpol.2017.11.064
503	Government of Canada. 2024. Canada Gazette, Part 1, Volume 158, Number 26: Regulations Respecting
504	the Reduction in the Release of Methane (Waste Sector). Government of Canada, Public Works and
505	Government Services Canada, Integrated Services Branch, Canada Gazette. https://gazette.gc.ca/rp-
506	pr/p1/2024/2024-06-29/html/reg5-eng.html
507	Hossain, RI, Buntov, P, Dudak, Y, Martino, R, Fougere, C, Naseridoust, S, Bourlon, E, Lavoie, M,
508	Khaleghi, A, Hall, C, Risk, D. 2025. A controlled release experiment for investigating methane

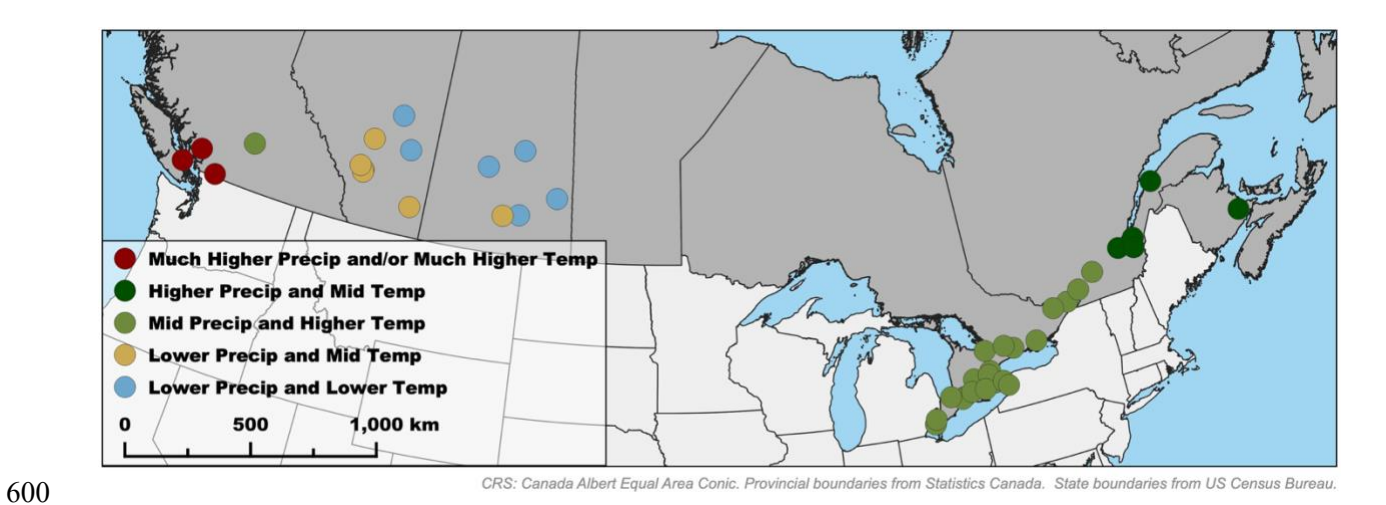
509 measurement performance at landfills [preprint]. Earth ArXiv. 510 https://eartharxiv.org/repository/view/8985/ 511 (IPCC) Intergovernmental Panel on Climate Change. 2006. 2006 IPCC Guidelines for National 512 Greenhouse Gas Inventories, Volume 4: Agriculture, Forestry and Other Land Use. IPCC National 513 Greenhouse Gas Inventories Programme. Eggleston HS, Buendia L, Miwa K, Ngara T, Tanabe K 514 (eds). Hayama 515 IPCC. 2000. Good Practice Guidance and Uncertainty Management in National Greenhouse Gas 516 Inventories - J Penman, D Kruger, I Galbally, T Hiraishi, B Nyenzi, S Emmanul, L Buendia, R 517 Hoppaus, T Martinsen, J Meijer, K Miwa and K Tanabe (Eds). ISBN 4-88788-000-6. 518 https://www.ipcc.ch/publication/good-practice-guidance-and-uncertainty-management-in-national-519 greenhouse-gas-inventories/ 520 Jain, P, Wally, J, Townsend, TG, Krause, M, Tolaymat, T. 2021. Greenhouse gas reporting data improves 521 understanding of regional climate impact on landfill methane production and collection. PLoS One 522 16(2): e0246334. https://doi.org/10.1371/journal.pone.0246334 523 Krause, MJ, Chickering, GW, Townsend, GT, Reinhart, DR. 2016. Critical review of the methane generation potential of municipal solid waste. Critical Reviews in Environmental Science and 524 525 Technology 46(13): 1117–1182. https://doi.org/10.1080/10643389.2016.1204812 526 Liland, KH. 2015. 4S Peak Filling – baseline estimation by iterative mean suppression. Methods X 2: 135– 527 140. https://doi.org/10.1016/j.mex.2015.02.009 528 Matacchiera, F, Manes, C, Beaven, RP, Rees-White, TC, Boano, F, Mønster, J, Scheutz, C. 2019. 529 AERMOD as a Gaussian dispersion model for planning tracer gas dispersion tests for landfill methane 530 emission quantification. Waste Management 87: 924-936. 531 https://doi.org/10.1016/j.wasman.2018.02.007

532	Mohsen, RA, Abbassi, B. 2020. Prediction of greenhouse gas emissions from Ontario's solid waste
533	landfills using fuzzy logic based model. Waste Management 102: 743-750.
534	https://doi.org/10.1016/j.wasman.2019.11.035
535	Omelchenko, M. V., Vasilyeva, L. V., & Zavarzin, G. A. (1993). Psychrophilic methanotroph from
536	tundra soil. <i>Current Microbiology</i> , 27(5), 255–259. https://doi.org/10.1007/BF01575988
537	Park, JR., Moon, S, Ahn, YM, Kim, JY, Nam, K. 2005. Determination of Environmental Factors
538	Influencing Methane Oxidation in a Sandy Landfill Cover Soil. Environmental Technology 26(1): 93
539	102. https://doi.org/10.1080/09593332608618586
540	Pipatti, R, Svardal, P. 2006. Solid waste disposal. In: Eggleston, S, Buendia, L, Miwa, K, Ngara, T.,
541	Tanabe K, editors. 2006 IPCC Guidelines for National Greenhouse Gas Inventories. Vol 5.
542	Intergovernmental Panel on Climate Change. http://www.ipcc-
543	nggip.iges.or.jp/public/2006gl/pdf/5 Volume5/V5 3 Ch3 SWDS.pdf
544	Risk, D, Omidi, A, Bourlon, E, Khaleghi, A, Perrine, G, Tarakki, N, Martino, R, Stuart, J. 2025. Active
545	face emissions: An opportunity for reducing methane emissions in global waste management
546	[preprint]. Earth ArXiv. https://eartharxiv.org/repository/view/8891/
547	Scarpelli, TR, Cusworth, DH, Duren, RM, Kim J, Heckler, J, Asner, GP, Thoma, E, Krause, MJ, Heins,
548	D, Thorneloe, S. 2024. Investigating major sources of methane emissions at US landfills.
549	Environmental Science and Technology 58(49): 21545–21556.
550	https://doi.org/10.1021/acs.est.4c07572
551	Scharff, H, Jacobs, J. 2006. Applying guidance for methane emission estimation for landfills. Waste
552	Management 26(4): 417–429. https://doi.org/10.1016/j.wasman.2005.11.015

- 553 Scheutz, C, Fredenslund, AM, Chanton, J, Pedersen, GB, Kjeldsen, P. 2011. Mitigation of methane
- emission from Fakse landfill using a biowindow system. *Waste Management* 31(5): 1018–1028.
- 555 https://doi.org/10.1016/j.wasman.2011.01.024
- Scheutz, C., & Kjeldsen, P. (2004). Environmental Factors Influencing Attenuation of Methane and
- Hydrochlorofluorocarbons in Landfill Cover Soils. *Journal of Environmental Quality*, 33(1), 72–79.
- 558 https://doi.org/10.2134/jeq2004.7200
- 559 Spokas, KA, Bogner, JE. 2011. Limits and dynamics of methane oxidation in landfill cover soils. Waste
- 560 Management 31(5): 823–832. https://doi.org/10.1016/j.wasman.2009.12.018
- Thompson, S, Sawyer, J, Bonam, R, Valdivia, JE. 2009. Building a better methane generation model:
- Validating models with methane recovery rates from 35 Canadian landfills. *Waste Management* 29(7):
- 563 2085–2091. https://doi.org/10.1016/j.wasman.2009.02.004
- Turner, DB. 1964. A diffusion model for an urban area. Journal of Applied Meteorology and Climatology
- 3(1): 83-91. https://journals.ametsoc.org/view/journals/apme/3/1/1520-
- 566 0450 1964 003 0083 admfau 2 0 co 2.xml
- Vu, HL, Ng, KTW, Richter, A. 2017. Optimization of first order decay gas generation model parameters
- for landfills located in cold semi-arid climates. *Waste Management* 69: 315–324.
- 569 https://doi.org/10.1016/j.wasman.2017.08.028
- Wang, Y, Fang, M, Lou, Z, He, H, Guo, Y, Pi, X, Wang, Y, Yin, K, Fei, X. 2024. Methane emissions
- from landfills differentially underestimated worldwide. *Nature Sustainability* 7(4): 496–507.
- 572 https://doi.org/10.1038/s41893-024-01307-9

5/4	Contributions
575	Contributed to conception and design: DR, SF, FV
576	Contributed to acquisition of data: JS, RM, LC, DR
577	Contributed to analysis and interpretation of data: EB, DR, JS, RM, LC, EL, NB, SF, SA, FV
578	Drafted and/or revised the article: JS, DR, EB, RM, LC, EL, NB, SF, SA, FV
579	Approved the submitted version for publication: DR, EB, JS, RM, LC, EL, NB, SF, SA, FV
580	Acknowledgments
581 582 583	We thank all landfill operators who facilitated our work. We also appreciate the contributions of the skilled Environment and Climate Change Canada staff in the Pollutant Inventories and Reporting Division, Climate Research Division, and Waste Reduction and Management Division.
584	Funding information
585 586	Funding for the study was made available by Environment and Climate Change Canada through a Contribution Agreement to St. Francis Xavier University.
587	Competing interests
588 589	The authors declare that there are no competing financial or personal interests in relation to the work described.
590	Supplemental material
591 592 593	S1 Quantification of methane sources using mobile plume transects. This describes the inversion approach based on the Gaussian Plume Model used to estimate methane emission rates from mobile measurements in this study.
594	PDF document, intitled "StFX_FluxLab_Canada_Landfills_Study_Elementa_SupplMat.pdf"
595	Data accessibility statement
596 597 598	The data presented in this study are available at https://doi.org/10.5683/SP3/PGJX03 . In this file, the landfill geolocation was removed to preserve site anonymity.

599 Figures



601 Figure 1. Locations of landfill sites.

The colors represent the climate categories based on precipitation amounts and mean temperatures from

603 2018 to 2022.

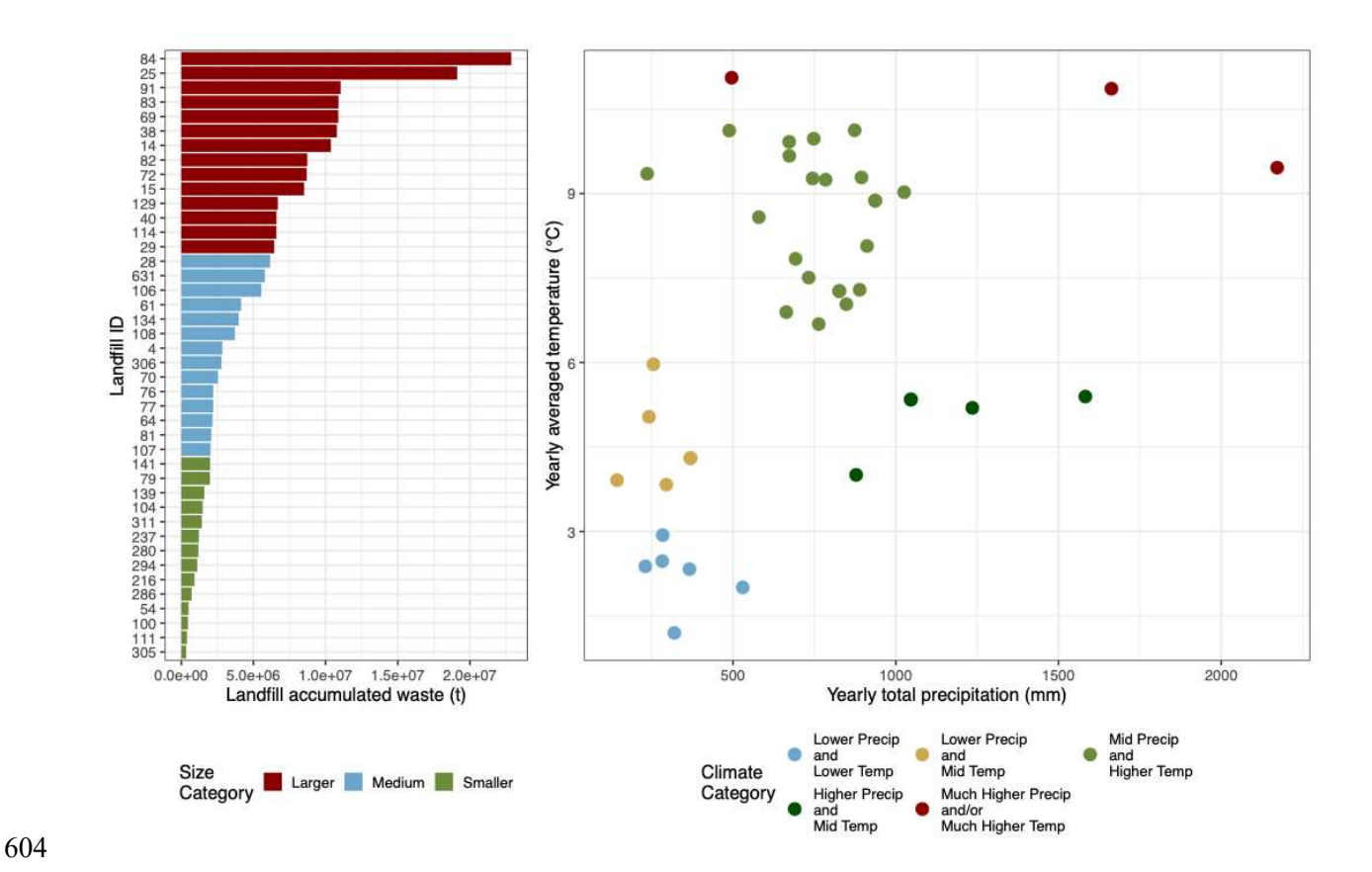


Figure 2. Landfill sizes and climate categories.

The left panel shows the distribution of landfill size, based on the accumulated waste tonnage as of 2022. Sizes were divided into 3 groups, and the colors of the bars indicate the size category of each landfill. The right panel represents the yearly average temperature (in °C) versus the yearly average precipitation amount (in mm) for each landfill. Both quantities were calculated using weather data from ECCC stations located within 50 km of each site. The colors indicate the climate clusters we used in this study.

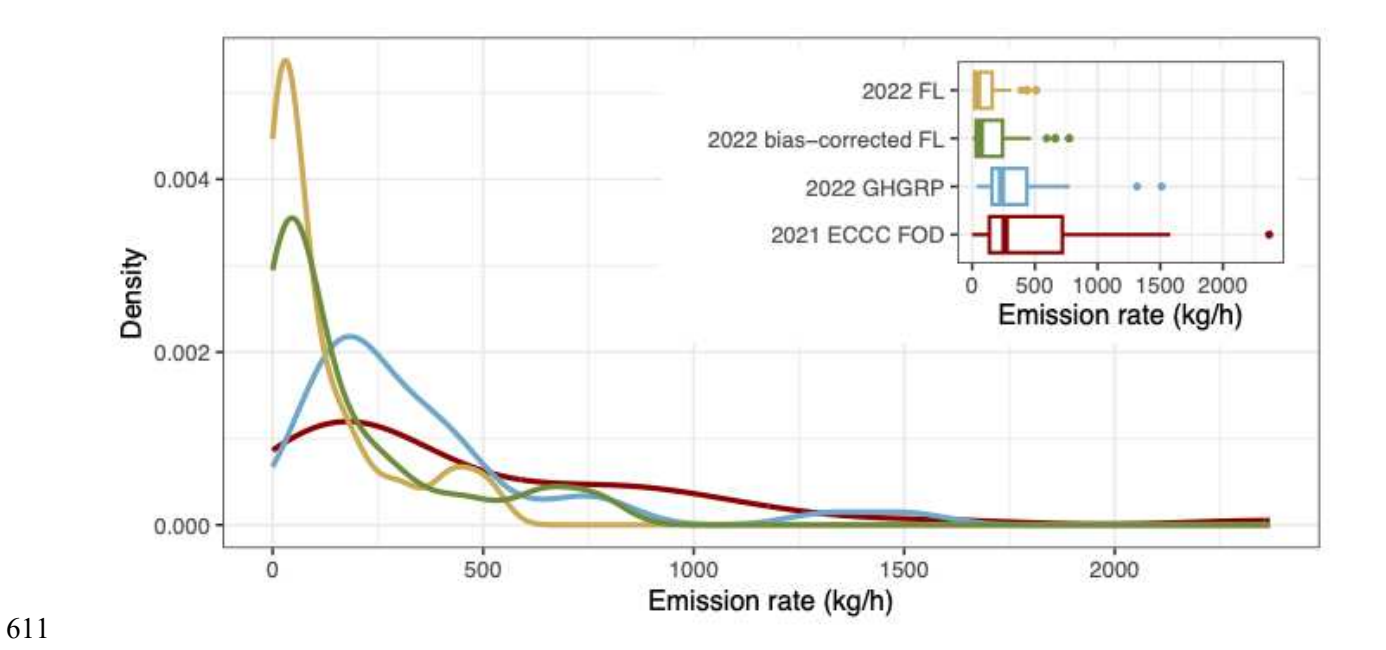


Figure 3. Density plot of landfill direct and bias-corrected measurement-based emission rate estimates, industry-reported GHGRP estimates, and ECCC FOD model estimates.

This figure highlights the difference in the distribution of each rate product. The inset illustrates how the range of each rate product compares to the others.

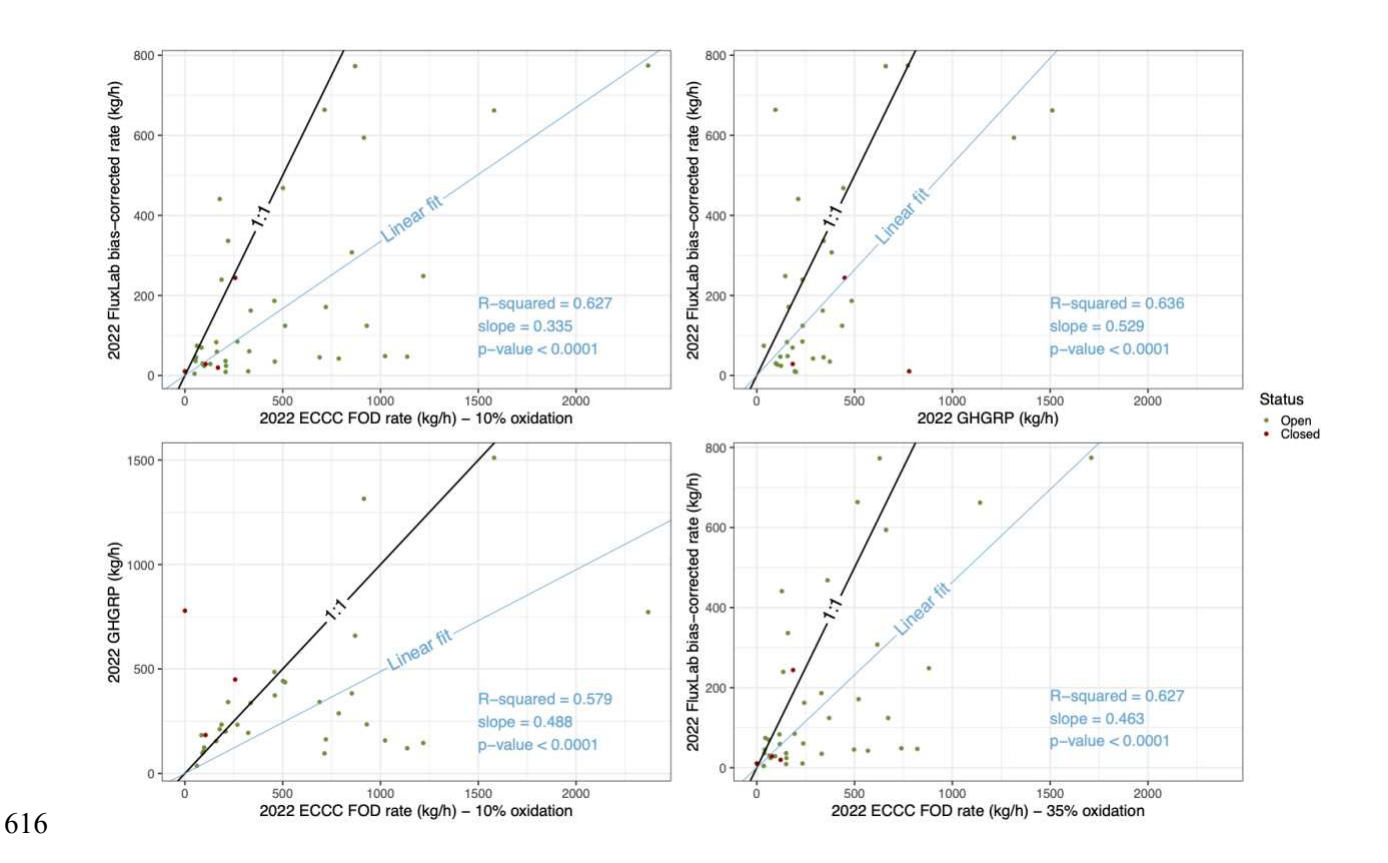


Figure 4. Linear regressions between the measurement-based rates, the ECCC modeled rates, and the GHGRP reported rates.

Left column: Measurement-based emission rate estimates (top) and GHGRP (bottom) versus ECCC FOD model estimates. Right column: Measurement-based estimates versus GHGRP (top) and versus ECCC FOD model with 35% methane oxidation (bottom). Note that the reported uncertainty for the IPCC FOD modeled rate, using the standard parameters, is $\pm 76\%$, while the uncertainty for measurement-based rates—estimated from the controlled release experiment—is 47.6%.

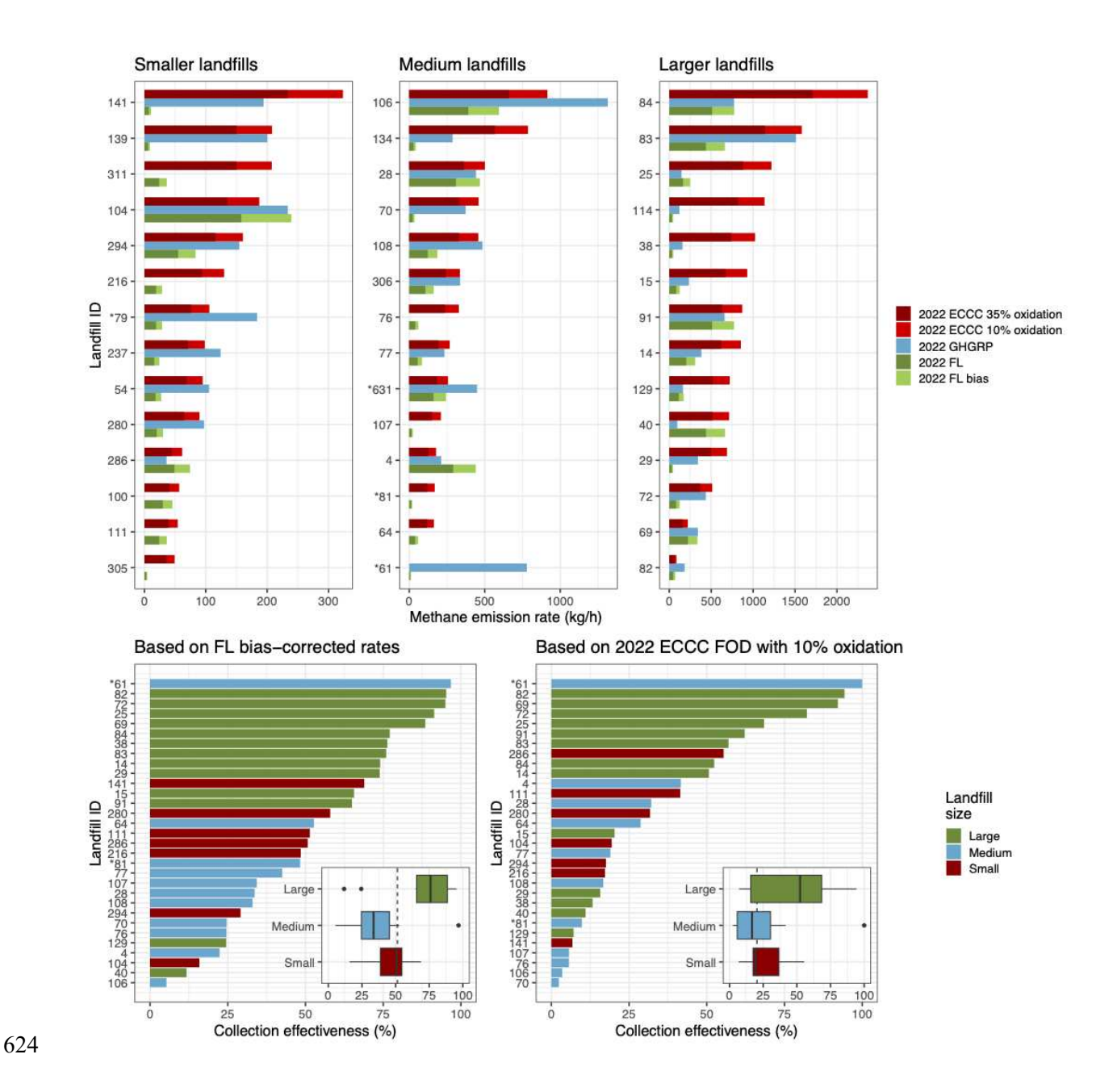


Figure 5. Methane emission rates and methane collection effectiveness.

Top row: Measurement-based emission rate estimates compared to ECCC FOD modeled rates (10% and 35% oxidation) and GHGRP values for closed and open landfills, sorted by decreasing ECCC rates.

Bottom row: Collection effectiveness based on measurement-based rates (left) and ECCC FOD modeled rates with 10% oxidation (right), ordered by increasing collection efficiency. The insets show the effectiveness by landfill size.

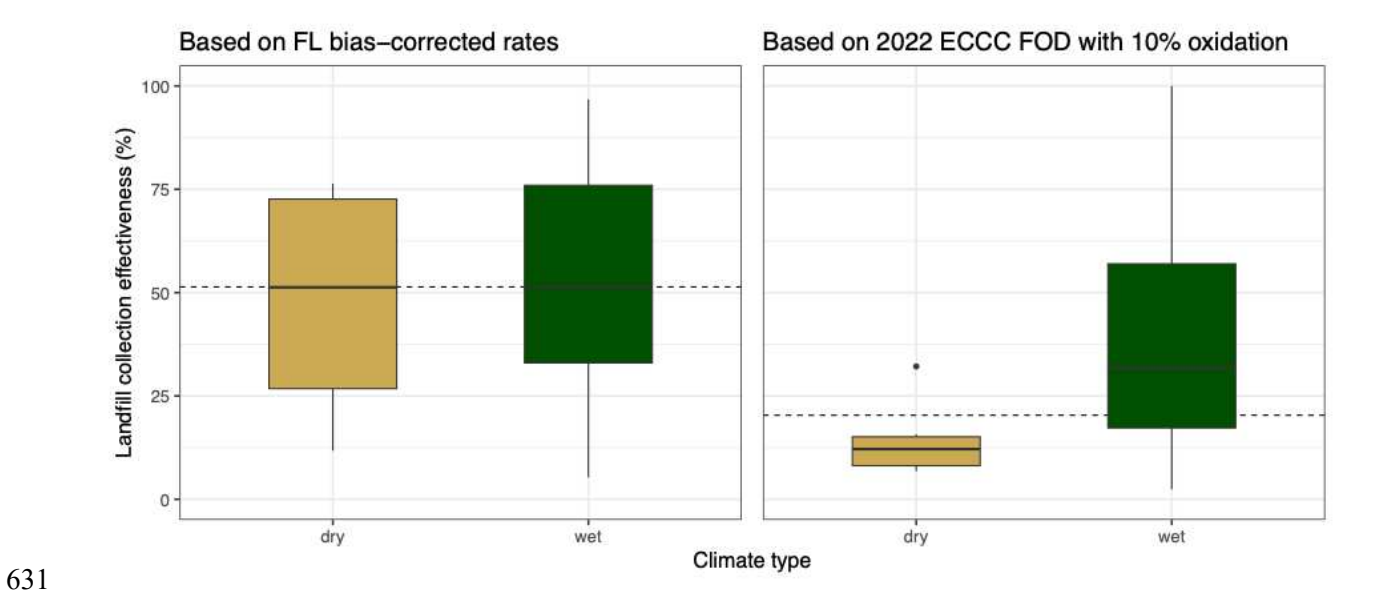


Figure 6. Collection efficiency per type of climate, based on measurement-based rate (left) and on ECCC FOD modeled rates (right).

The "dry" type combines the two lower precipitation categories, and the "wet" one comprises the mid, high, and higher precipitation climate categories. Efficiencies estimated using measurement-based rates show no relationship with climate. In contrast, efficiencies from the FOD modeling reveal a sharp difference between dry and wet climates.

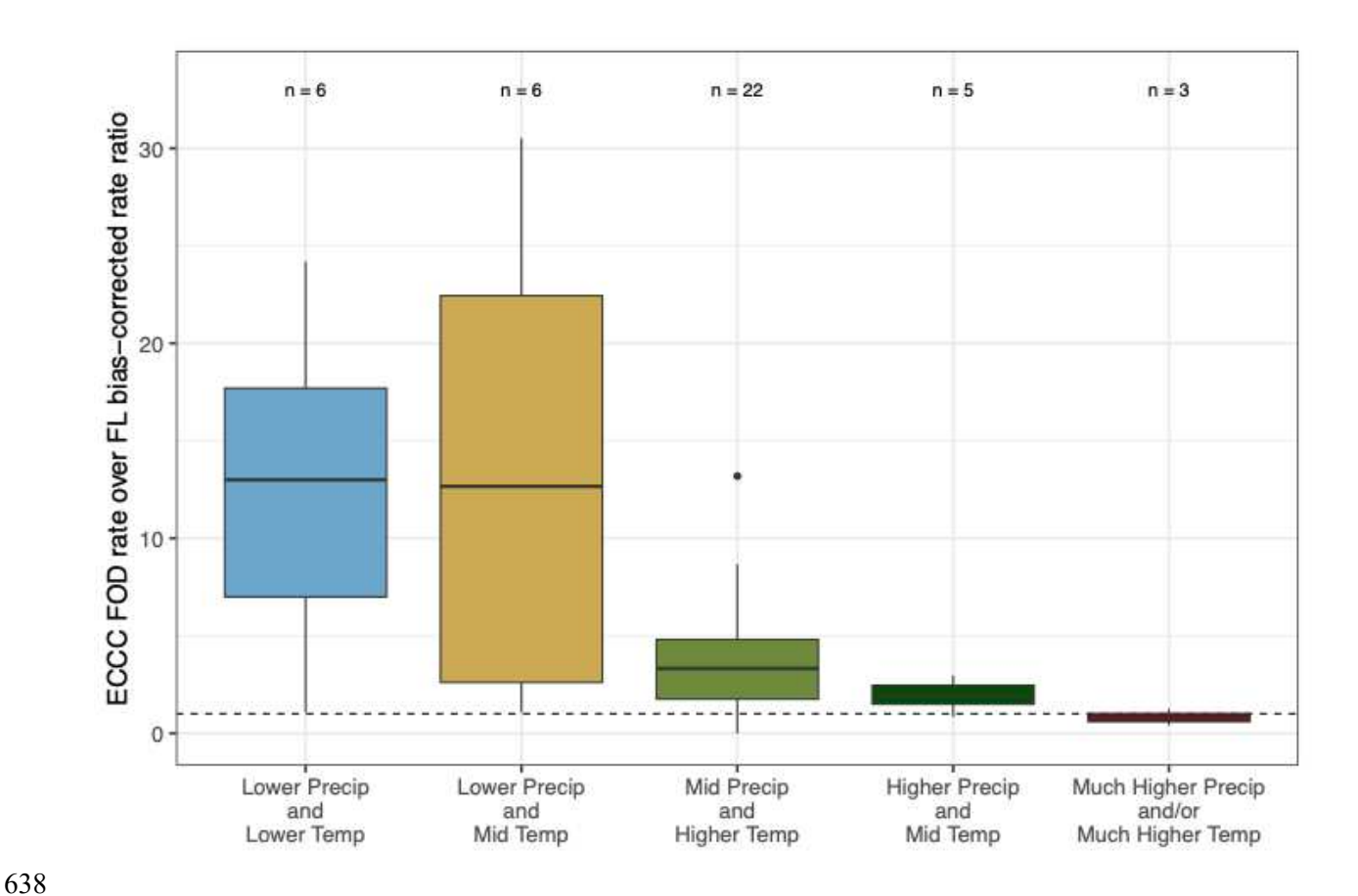


Figure 7. Ratio of measurement-based to ECCC FOD-modeled rate estimates across climate categories.

This figure highlights the amplitude of the difference between measurement-based rates and ECCC modeled rates. The dashed line represents the 1:1 ratio. When boxes are above this line, ECCC rates are higher than the measurement-based rates, and when ECCC rates are lower than the measurement-based rates. The numbers on top of the boxes indicate the number of landfills in each climate category.

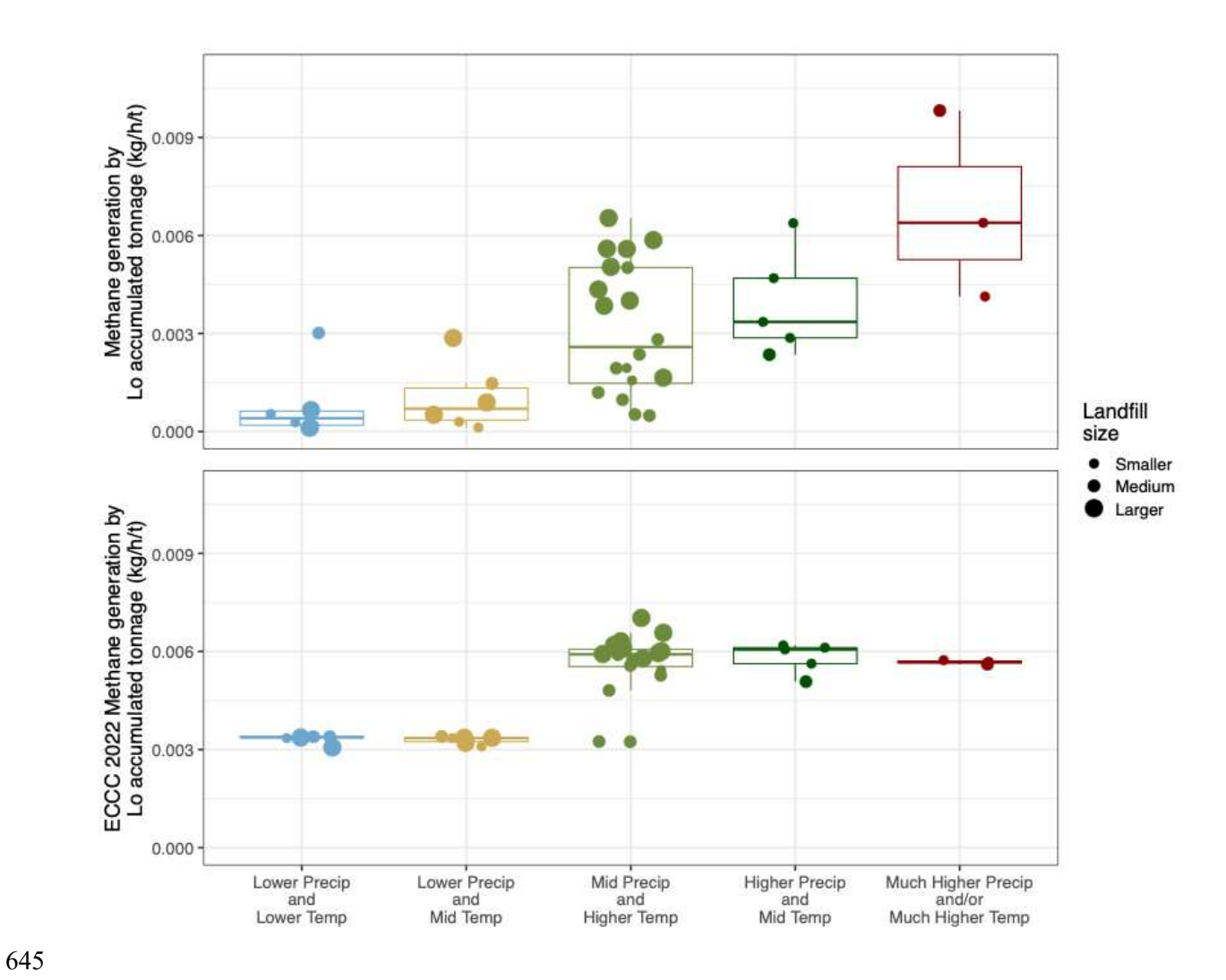


Figure 8. Relation between methane generation per methane potential (L_0 accumulated tonnage) and climate zone.

In the top plot, the methane generation was calculated using 2022 reported collection volumes and 2022 measurement-based methane emissions. The 2022 methane generation rate from the ECCC FOD modeling is used in the bottom plot.

652 Tables

Table A. Bulk landfill waste decay rates (k in y⁻¹) per climate categories based on our emission rate measurement and FOD modeling.

Waste degradation depends on several factors, including moisture and temperature. Therefore, this table also presents the median annual precipitation and median annual temperature for each climate category. The median k values are reported with their second and third quartile ranges (Median [2^{nd} quartile – 3^{rd} quartile]).

Climate category	Median precipitation (mm)	Median annual temperature (°C)	Measurement-based decay rate k (y ⁻¹)	FOD-based decay rate k (y ⁻¹)
Lower Precip and Lower Temp	302	2.4	0.004 [0.002-0.006]	0.030 [0.030-0.030]
Lower Precip and Mid Temp	275	4.3	0.007 [0.003-0.014]	0.030 [0.028-0.030]
Mid Precip and Higher Temp	774	8.9	0.024 [0.013-0.046]	0.053 [0.049-0.055]
Higher Precip and Mid Temp	1046	5.3	0.032 [0.027-0.044]	0.055 [0.051-0.055]
Much Higher Precip and/or Much Higher Temp	1663	10.9	0.063 [0.052-0.081]	0.051 [0.051-0.051]

1	Supplementary Material
2	for
3	Canada's Landfill Methane Inventories: The Challenge of Accurate Modeled and
4	Measurement-Based Emissions
5	Jordan Stuart ¹ , David Risk ^{1,*} , Evelise Bourlon ¹ , Rebecca Martino ¹ , Lindelwa Coyle ¹ , Emil Laurin ² ,
6	Nicholas Bishop ² , Susan Fraser ² , Sebastien Ars ² , Felix Vogel ²
7	¹ FluxLab, Department of Earth and Environmental Sciences, St. Francis Xavier University, Nova Scotia,
8	Canada
9	² Environment and Climate Change Canada, Ontario, Canada
10	*Corresponding author: David Risk drisk@stfx.ca
11	Publication in Elementa—Science of the Anthropocene
12	October 3 rd , 2025
13	

14	Contents
14	Comenis

15	S1 Quantification of methane sources using mobile plume transects	
16	Gaussian plume dispersion model and assumptions	
17	Gaussian Plume Inversion	
18	The damping effect of the gas sensor on the methane measurement	
19	Inversion approach	
20	Figures	
21	References	
22		
23	Figure S1. Two examples of field data comparison.	
24	Figure S2. Comparison plots of our measured area versus each of the ECCC measured areas over	
25	multiple transects.	
26	Figure S3. Illustration of the result from a laboratory measurement of our Picarro 2210i signal	
27	damping.	
28		

S1 Quantification of methane sources using mobile plume transects

31 Gaussian plume dispersion model and assumptions

- Numerous experimental field studies have been conducted to investigate the passive dispersion of non-
- reactive pollutants from continuous point sources, providing a foundation for the work of Sutton (1953)
- and Pasquill (1962). One important empirical feature is that the time-averaged concentration profiles are
- 35 Gaussian in both the horizontal and vertical directions. The Pasquill-Gifford Gaussian plume model
- 36 predicts concentrations from the distance to the source location, source height, source emission rate, wind
- speed, and dispersion coefficient. In this model, the pollutant is entirely reflected by the ground surface.
- Using a mathematical reference frame where the x axis is the downwind direction, the y axis the
- crosswind direction, and the z axis the vertical direction positive upward, the concentration χ (in µg/m3)
- in (x, y, z) for a continuous elevated point source located in (x_s, y_s, h) is:

$$\chi(x,y,z) = \frac{Q}{2\pi\sigma_y\sigma_z u} \times exp\left(-\frac{(y-y_s)^2}{2\sigma_y^2}\right) \times \left\{exp\left[\frac{-(z-h)^2}{2\sigma_z^2}\right] + exp\left[\frac{-(z+h)^2}{2\sigma_z^2}\right]\right\}$$
(1)

- 41 where σ_v and σ_z are the dispersion parameters (in m) in the crosswind and downwind direction, resp., u is
- 42 the wind speed (in m/s), h is the source height (in m), and Q is the emission rate (in μ g/s). The
- 43 concentration γ is implicitly a function of x through the dispersion parameters. These parameters describe
- the horizontal and vertical spread of the plume, and their equations (known as the σ -functions) were
- 45 derived by Turner (1970) by fitting the Pasquill-Gifford curves (Gifford, 1961) for open country settings.
- 46 The dispersion equations are keyed to the atmospheric stability classes that express the ratio of buoyancy
- 47 over mechanical turbulence. Class A corresponds to the most unstable conditions, class D to neutral
- 48 conditions, and class F to the most stable conditions. The turbulence intensity increases under unstable
- 49 atmospheric conditions with the development of vertical air parcel updrafts, and it is reduced under stable
- atmospheric conditions that suppress those vertical updrafts. There are several atmospheric stability
- 51 classification schemes, and they require a variable number of meteorological variables. The Pasquill
- 52 classification (Pasquill, 1961) only requires the wind speed and an estimate of the solar radiation. In this

study, we utilized a classification by Tuner (1964), where the Pasquill scheme is refined by determining an index of solar radiation using the solar elevation angle (calculated using the location and the time) and the cloud cover and ceiling height, both standard weather measurements at most weather stations. The Gaussian plume model assumes continuous emission at a constant rate and constant meteorological conditions at least over the time of transport from the source to the sensor. The effect of plume rise at the source is not considered, but the effective height can replace the source height in the equation. The Gaussian plume model should not be applied under conditions of low wind speed (< 1m/s), and the equation presented here does not account for complex terrain, or deposition and chemical reaction within the plume during travel from the source to the sensor.

62 Gaussian Plume Inversion

From Equation 1, the concentration from one source at one location (x, y, z) is linearly proportional to the source emission rate Q:

$$\chi(x, y, z) = Q \times \frac{\chi_{Q_1}(x, y, z)}{Q_1} = Q \times c(x, y, z)$$
(2)

where χ_{Q1} is the concentration for an emission rate of Q₁ and c is the concentration from a source with a unitary emission rate (1 g/s). Each concentration measurement leads to one emission rate. A joint inversion of several concentration measurements can be performed to obtain a single emission rate. In matrix form, we have to solve:

$$\chi = \begin{bmatrix} \chi_1 \\ \chi_2 \\ \vdots \\ \chi_n \end{bmatrix} = Q \times \begin{bmatrix} c_1 \\ c_2 \\ \vdots \\ c_n \end{bmatrix}$$
 (3)

where χ is the vector of measured concentrations at locations 1 to n, Q is the emission rate, and c is the vector of concentration for a 1g/s emission rate at the same n locations. This can be generalized for multiple emitting sources. The total measured concentration is the sum of each source contribution, and equation (3) can be rewritten as

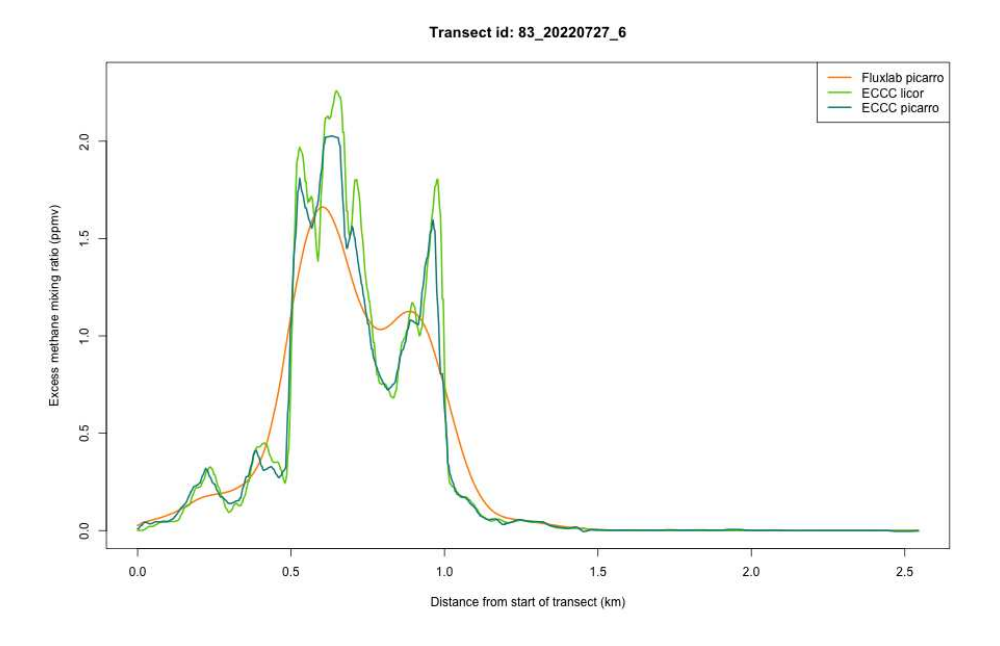
$$\chi = \begin{bmatrix} \chi_1 \\ \chi_2 \\ \vdots \\ \chi_n \end{bmatrix} = Q_1 \times \begin{bmatrix} c_{11} \\ c_{12} \\ \vdots \\ c_{1n} \end{bmatrix} + Q_2 \times \begin{bmatrix} c_{21} \\ c_{22} \\ \vdots \\ c_{2n} \end{bmatrix} + \dots + Q_m \times \begin{bmatrix} c_{m1} \\ c_{m2} \\ \vdots \\ c_{mn} \end{bmatrix}$$
(4)

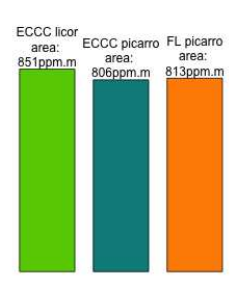
73 or

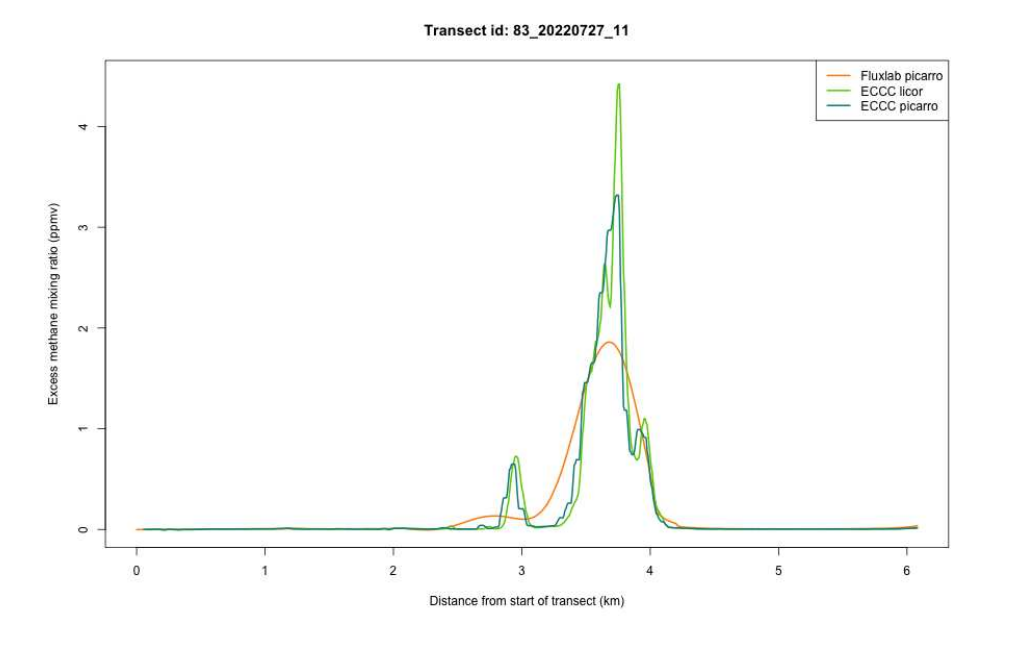
$$\chi = qC \tag{5}$$

- where q is a vector of point emission rates from source 1 to m and C is an n×m matrix of concentration
- 75 from source 1 to m, for a rate of 1g/s and measurement locations 1 to n.

- 77 The damping effect of the gas sensor on the methane measurement
- 78 The response of cavity ring-down instruments, such as the ones we used in our mobile survey setting, to
- an increase in methane varies with their flow rate and cavity size. We compared the height and area of the
- 80 methane enhancements recorded by several analyzers that were sampling simultaneously, both in the
- laboratory (Figure S3) and in the field (Figure S1). We found that while slower instruments tend to damp
- peaks relative to faster ones, the areas of the peaks were similar for all instruments (Figure S2). Therefore,
- 83 we used the integrated methane measurement as our data constraint in the inversion.
- 84 Inversion approach
- 85 We want to minimize the difference between γ and qC, with the constraint that all the elements of q are
- 86 positive, since our input locations are sources of methane, and not sinks. We solve this problem using
- 87 NonNegative Least Squares optimization:
- 88 $min_q \parallel qC \chi \parallel^2 \text{ subject to } q \geq 0.$
- We use the R interface to a Fortran 77 code by Lawson and Hanson (1995), based on the algorithm
- 90 described by Lawson and Hanson (1974).







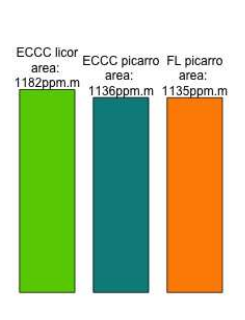


Figure S1. Two examples of field data comparison.

The plots on the left show the methane measurements, corrected for the ambient methane level, from three instruments installed in two mobile laboratories conducting simultaneous surveys at the same location. The ECCC mobile laboratory was equipped with a Licor LI810 and a Picarro G1301. Our setting

includes a Picarro 2210i, with a slower response than both ECCC instruments. The bars on the right show that, independent of the response of the instrument, the area under the curve is unchanged.

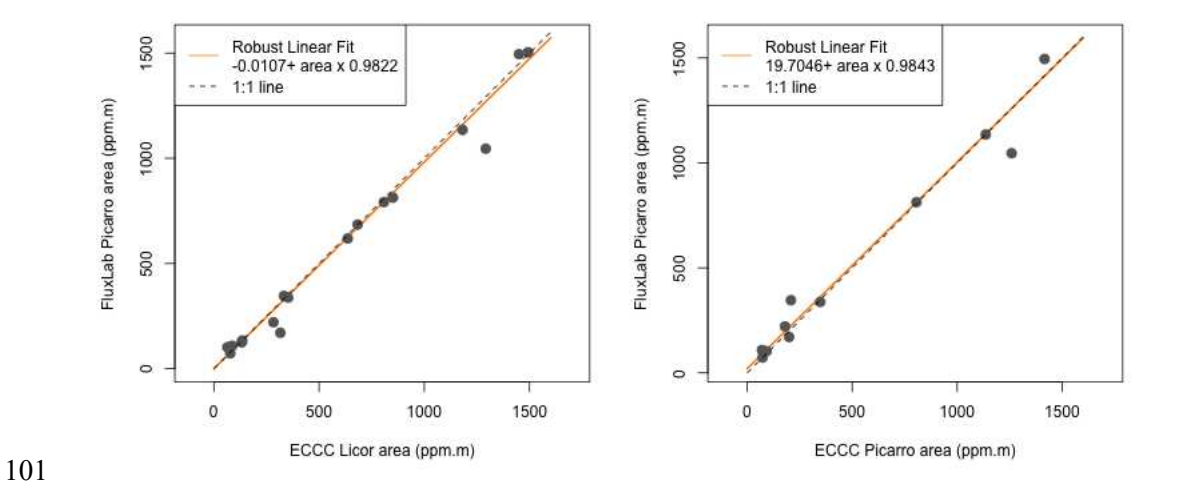


Figure S2. Comparison plots of our measured area versus each of the ECCC measured areas over multiple transects.

Left panel: ECCC Licor vs FluxLab Picarro concentration area. Right panel: ECCC Picarro vs FluxLab Picarro concentration area. Both fits are close to the 1:1 line.

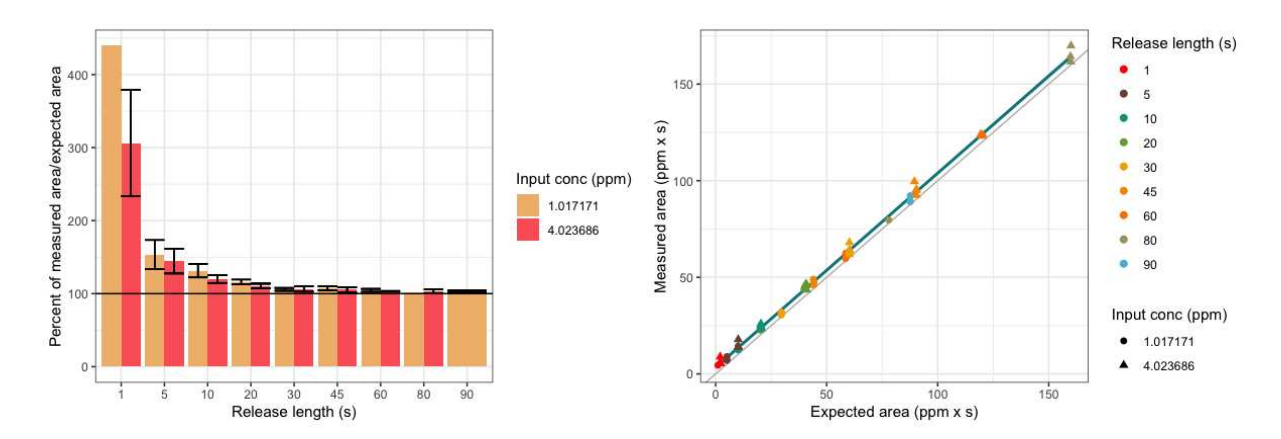


Figure S3. Illustration of the result from a laboratory measurement of our Picarro 2210i signal damping.

109 Timing and length of release were measured, and we used 2 methane cylinders: one at 4ppmy (~2ppmy 110 above ambient) and one at 1ppmv (~1ppmv below ambient). Left panel: Measured area as a percentage of 111 the expected area versus the release duration. Right panel: Measured area versus expected area. The curve 112 integration/area is overestimated by a factor of 3 to 4 for 1s-long releases, but the overestimation is below 113 20% when the release is longer than 20s. The stretching of the anomaly seems to compensate for the 114 damping of its amplitude. 115 References 116 117 Gifford, F. 1961. Use of Routine Meteorological Observations for Estimating Atmospheric Dispersion. 118 Nuclear Safety, 2, 44-57. 119 Lawson CL, Hanson RJ. 1974. Solving Least Squares Problems. Prentice Hall, Englewood Cliffs, NJ. 120 Lawson CL, Hanson RJ. 1995. Solving Least Squares Problems. Classics in Applied Mathematics. 121 SIAM, Philadelphia. 122 Pasquill, F. 1961. The Estimation of the Dispersion of Windborne Material. Meteorology Magazine, 90, 33-40. 123 124 Pasquill, F. 1962. Atmospheric diffusion, Quarterly Journal of the Royal Meteorological Society, 125 Vol.88(376), https://doi.org/10.1002/qj.49708837622

Turner, DB. 1964. A Diffusion Model for an Urban Area, Journal of Applied Meteorology and Climatology, Vol.3(1), Pages 83-91, https://doi.org/10.1175/1520-

Sutton, OG. 1953. Micrometeorology, Quarterly Journal of the Royal Meteorological Society,

130 0450(1964)003%3C0083:ADMFAU%3E2.0.CO;2

Vol.79(341), https://doi.org/10.1002/qj.49707934125

126

- Turner, DB. 1970. Workbook of atmospheric dispersion estimates (Rev). U.S. Dept. of Health Education
 and Welfare, Public Health Service, Environmental Health Service, National Air Pollution Control
- 133 Administration.